

HL-LHC BEAM DYNAMICS WITH HOLLOW ELECTRON LENSES

P. D. Hermes*, R. Bruce, R. De Maria, M. Giovannozzi, A. Mereghetti†, D. Mirarchi, S. Redaelli
 CERN Beams Department, Geneva, Switzerland
 G. Stancari

Fermi National Accelerator Laboratory, Batavia, Illinois, USA

Abstract

Each of the two proton beams in the High-Luminosity Large Hadron Collider (HL-LHC) will carry a total energy of 700 MJ. One concern for machine protection is the energy stored in the transverse beam halo, estimated to potentially reach up to 5% of the total stored energy. Several failure scenarios could drive this halo into the collimators, potentially causing damage and therefore severely affecting operational efficiency. Hollow Electron Lenses (HEL) were integrated in the HL-LHC baseline to mitigate this risk by depleting the tails in a controlled way. A hollow-shaped electron beam runs co-axially with the hadron beam over about 3 m, such that halo particles at large amplitudes become unstable, while core particles ideally remain undisturbed. Residual fields from electron beam asymmetries can, however, induce emittance growth of the beam core. Various options for the pulsing of the HEL are considered and are compared using two figures of merit: halo depletion efficiency and core emittance growth. This contribution presents simulations for these two effects with different HEL pulsing modes using updated HL-LHC optics, that was optimized at the location of the lenses.

INTRODUCTION

Small fractions of the large stored beam energy in HL-LHC [1] can potentially cause severe damage to the machine hardware and negatively impact the operational efficiency, if they are lost in an uncontrolled way. The Large Hadron Collider (LHC) [2] is already equipped with a sophisticated, multi-stage collimation system [3–5] to intercept particles at large betatron or momentum offsets before they are lost in the sensitive LHC hardware. The highly-populated beam halo poses additional concerns that the upgraded HL-LHC collimation system [6] might not be able to cope with.

Assuming that up to 5% of the stored beam energy can be located in the halo of the circulating proton beams [7, 8], some of the failure scenarios that may occur in HL-LHC [9, 10] put at risk the integrity of the collimation system itself, with potentially severe consequences for the scientific programme. Most notably, for the context of this work, machine safety is endangered by sudden orbit shifts which would steer the highly populated beam halo into the primary collimators, that are closest to the circulating beams. Overall, the collimation system must work safely, also with sudden orbit shifts in the order of 2σ (with σ being the RMS beam size).

Hollow electron lenses (HEL) have recently been added to the upgrade baseline of the HL-LHC [6] to mitigate effects of highly-populated beam halo through an active control of its halo population. This paper reviews the key parameters of the HELs and gives a status update of the beam dynamics simulations for the halo depletion efficiency and the impact of residual fields on the emittance of the beam core.

HOLLOW ELECTRON LENSES FOR HL-LHC COLLIMATOR

Hollow Electron Beam Parameters

The HEL [11] is a device that can actively remove particles at large transverse amplitudes, and thus deplete the halo in a controlled way. For this purpose, a hollow-shaped electron beam (see Fig. 1) is created and guided through a magnetic system in which the hadron and electron beams run co-axially over a certain length. The electron beam distribution is characterized by an inner and outer radius r_1 and r_2 , respectively. Hadron particles moving through the HEL with a transverse amplitude smaller than r_1 are ideally unaffected, because the net electric and magnetic fields generated by the surrounding electron current yield zero. Hadrons with larger amplitudes than r_1 are subject to electric and magnetic fields which change their transverse momentum. This kick $\theta(r)$ is a function of the radius $r = \sqrt{x^2 + y^2}$ of the particle and can be quantified as follows

$$\theta(r) = f(r) \theta_{\max} \left(\frac{r_2}{r} \right), \quad (1)$$

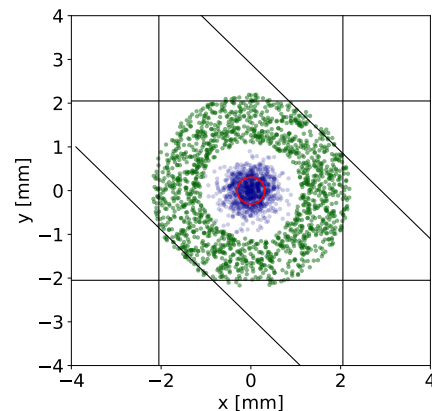


Figure 1: Transverse distribution of the hollow electron beam (green) and the hadron beam (blue) at the HEL. The black lines indicate the cut generated by the primary collimators. The red circle corresponds to one RMS beam size.

* pascal.hermes@cern.ch

† Currently at Fondazione CNAO, Strada Campeggi 53, 27100 Pavia, Italy

where $f(r)$ is an amplitude-dependent shape function corresponding to the fraction of the total electron current enclosed by a cylinder of radius r :

$$f(r) = \begin{cases} 0 & r < r_1 \\ \frac{r^2 - r_1^2}{r_2^2 - r_1^2} & r_1 \leq r \leq r_2 \\ 1 & r > r_2 \end{cases} . \quad (2)$$

While HELs can be used for all types of hadron beams that can be stored in HL-LHC, it is crucial for the operation of proton beams, which is why the following description will refer to protons instead of hadrons in general. All parameters of the HEL other than the inner and outer radii are subsumed in the maximum scattering angle θ_{\max} given by

$$\theta_{\max} = \frac{1}{4\pi\epsilon_0 c^2} \frac{2L I_e (1 \pm \beta_e \beta_p)}{(B\rho)_p \beta_e \beta_p r_2} , \quad (3)$$

where L is the active length of the HEL, I_e is the total electron-beam current, β_e and β_p are relativistic β -factor of the electrons and protons, respectively, and $(B\rho)_p$ is the magnetic rigidity of the proton beam. It is noteworthy that the transverse kick experienced by a particle increases linearly with the HEL length and the electron beam current. Furthermore, the two possible signs that can be taken by the \pm in the numerator correspond to the electrons moving in the same direction as the proton beam (-) or in the opposite one (+). Maximising θ_{\max} can obviously be reached by letting the electron beam move in the opposite direction with respect to the proton beam and by maximizing L and I_e .

With realistic electron beam parameters, values for θ_{\max} are typically in the order of some 0.1 μrad for 7 TeV proton beams. Several passages through the HEL are therefore required, before a particle is eventually lost in the collimators. The HEL thus induces a comparably slow transverse diffusion, which also ensures that the machine hardware is not endangered by a rapid beam loss created by the HEL itself.

For machine protection purposes, it is also important to keep the possibility to detect orbit drifts with the beam loss monitors at the HL-LHC collimators early enough to trigger a beam dump. For this purpose, a small fraction of the beam halo must be preserved and it is foreseen to leave several bunches of the proton beam unaffected by the HEL. For these so-called witness bunches, the electron beam is always switched off.

Residual Effects on the Beam Core

In the previous section, it was assumed that all particles at $r < r_1$ are not subject to a change of transverse momentum due to the electron lens. This applies to the idealized model of a perfectly symmetric electron beam. In reality, a residual field will act also on particles in the beam core, due to asymmetries in the transverse distribution of electrons. In the design specifications of the HEL [12], it is defined that the residual fields acting on particles in the beam core must not exceed a level that introduces a transverse dipole kick of

$$\Delta\theta_{\text{core}} = 1 \text{ nrad} . \quad (4)$$

A proton beam moving through the electron lens without the electron beam being present will receive no kick.

Pulsing of the HEL

Operating the HEL at constant current (i.e. the same electron current is applied at every turn for the non-witness bunches) is not expected to deliver sufficient depletion of the beam halo. Better efficiency of the halo depletion can potentially be reached by using turn dependent pulsing schemes. The following schemes have been studied [13]:

Constant-current mode: HEL is switched on at every turn with the same current I_e .

Pulsed mode P_i^j : HEL is switched on for i turns with constant current I_e and switched off for j turns.

Random mode R_p : HEL is switched on and off randomly at every turn with a certain probability p to be switched on and $1 - p$ to be switched off. If the HEL is switched on, the current is always equal to a constant value I_e .

Beam Dynamics Measures of HEL Performance

We measure the depletion performance of the HEL in terms of the percentage of depleted halo after a given period of time. The target depletion fraction is specified as removing 90% of the transverse halo within 5 minutes of HEL operation. Previous studies demonstrated that the operation of the HEL is the most efficient, i.e. the beam halo is removed fastest, if the electron beam is randomly switched on and off at every turn [11, 13]. This observation is expected, given the broad spectrum of frequencies that this mode of operation covers and it would be ideal for a perfect-HEL scenario with no residual field in the area $r < r_1$. In reality, this condition is not achievable and any residual component can perturb the proton beam dynamics.

In general, the non-symmetries of the electron beam introduce all orders of electromagnetic fields. The effect of the lowest order (dipolar) field is studied here. Studies with the effect of higher order field components are currently ongoing. Considering a residual kick θ_{core} , the operation in the random mode introduces random dipolar noise to the particles in the beam core. Such a noise diffuses particles from the beam core to larger amplitudes and thus increases the RMS beam emittance, with detrimental effects on the collider's luminosity. This undesired effect is quantified in terms of the emittance change $\Delta\epsilon$ per unit time.

UPDATED OPTICS AT THE HEL

In the current phase of preparing the implementation of the HL-LHC, the envisaged beam optics for HL-LHC are regularly updated, based on revised requirements and new knowledge gathered via simulations and LHC operation. The current optics version (referred to as V1.4, compared to the previous version V1.3) integrates optimised local optical

functions at the HEL location in order to obtain larger beam sizes and round optics, i.e. same β -functions in x and y [11]. Table 1 shows a comparison between the previous optics V1.3 and the updated optics V1.4, illustrating that the β -function increases by 42% in x and 32% in y .

Table 1: Optical functions at the location of the HEL for B1 of HL-LHC in Version 1.3 and the newer version 1.4, optimized at the location of the HEL.

Optics Version	V1.3	V1.4
β_x (m)	197.5	280.0
β_y (m)	211.9	280.0
α_x	0.98	0.64
α_y	-0.13	-0.25
$D_{x/y}$ (m)	0	0

The larger β -functions allow using a larger electron beam with the same normalized proton beam size. With larger electron beam size, the stability of the electron beam is increased and the tolerances for the device are more relaxed. On the other hand, it is expected that the effect of emittance growth due to the residual dipole field increases. Moreover, the efficiency of halo depletion in the different pulsing patterns can be affected by the change of machine optics. The studies presented in [11], carried out for V1.3, are therefore compared to a new set of simulations for V1.4 in the following sections.

SIMULATIONS OF HEL PERFORMANCE

For the comparison of the HEL performance with different optics, we use the same beam parameters and setup of non-linear elements as in the study presented in [13]. The most important key parameters are summarized in Table 2. Note that beam-beam interactions are not taken into account to assess the HEL performance, since it is intended to be operated after the acceleration ramp. This configuration is more challenging because it is expected that the non-linearities from beam-beam interactions would make the depletion more efficient. The β^* simulated corresponds to the operational configuration with squeezed but separated beams, right before collision. This was chosen for comparability to previous studies [13] and simulations with the configuration right after the acceleration ramp are going to be performed in the future.

As a case study, we take $r_1 = 5\sigma$ and $r_2 = 10\sigma$, using an electron current of 5 A with electrons of 10 keV and a HEL length of $L = 3$ m. Note that for the asymmetric β -functions in V1.3 the inner radius corresponds to 5σ in the horizontal plane, only. The residual kick deemed to have an effect on the beam core is $\theta_{\text{core}} = 1$ nrad in the vertical direction (where stronger asymmetries are expected from electron beam dynamics simulations [14]). It corresponds to the maximum residual field defined in the HEL design specifications.

While the simulations presented in [13] were carried out with SixTrack [15–17], the halo depletion simulations presented here were obtained by means of the new simulation tool XSuite, a development based on SixTrackLib [18, 19]. Both tools provide second-order symplectic tracking, taking into account multipole errors in the various magnetic elements of the ring. The emittance-growth simulations presented here were both carried out with SixTrack. Due to the long times needed for the tracking simulations, the emittance growth simulations were performed for only 2 million turns in HL-LHC (corresponding to almost 3 minutes in the collider) and the depletion simulations were limited to 60 s in the collider for constant current and random excitations. Pulsed operation was simulated 400 times for each optics with different periodicities, which is why we limited the simulated time in the collider to 10 s.

HEL Performance for Halo Depletion

We define the circulating halo n_{halo} as the amount of particles circulating at amplitudes between the inner radius of the electron beam in the HEL and the primary collimator (TCP) half gap at 6.7σ . We distinguish between the beam halo without HEL, n_{halo}^0 , and the beam halo with the HEL for a given pulsing pattern, $n_{\text{halo}}^{\text{HEL}}$, and we define the depletion fraction \mathcal{R}_d as

$$\mathcal{R}_d = 1 - \frac{n_{\text{halo}}^{\text{HEL}}}{n_{\text{halo}}^0}. \quad (5)$$

The initial distribution used for all simulations was sampled as a double Gaussian composed of one Gaussian with sigma equal to 1σ contributing 65% to the total, and another one with sigma equal to 2σ contributing 35%, to imitate the over-populated tails observed in the machine [20]. Each simulation considers 30000 initial particles.

Constant current mode The depletion fraction in the operation of the HEL with the constant-current pulsing mode, shown in Fig. 2 differ approximately by a factor of two, but are at low levels for both optics studied. After one minute of operation in constant current mode, approximately 1.4% of the halo has been depleted in HL-LHC V1.4, compared to 2.8% in V1.3. The difference is potentially related to

Table 2: Simulation parameters used in the numerical simulations. Q' corresponds to the chromaticity, I_{oct} to the current powering the Landau octupoles, the TCP half gap is the half gap of the primary collimators.

Parameter	Value
Beam	B1
β^* (IR1/IR5)	15 cm
Q'	15
I_{oct}	-300 A
TCP half gap	6.7σ

the smaller kick the particles receive with the larger relative electron beam size in the updated optics version.

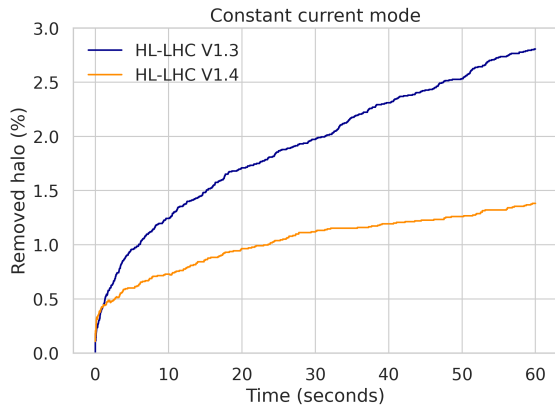


Figure 2: Halo depletion rate in the constant current mode for HL-LHC V1.3 and HL-LHC V1.4.

Random mode The simulated depletion efficiency in random mode is compared in Fig. 3. Note the change of scale compared to Fig. 2. In both cases the depletion is significantly more efficient than with the constant-current mode. The level of depletion reached after one minute of operation is 68% for HL-LHC Version 1.3 and 62% for HL-LHC version 1.4. The probability of switching the HEL on or off is 50% at each turn for both optics. While the final depletion fraction achieved is slightly different for the two cases, the depletion curve with time shows a similar shape.

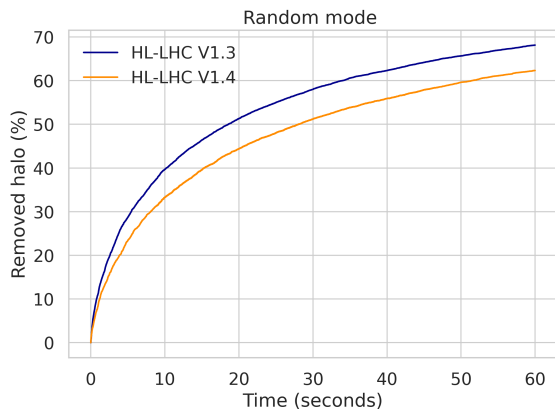


Figure 3: Comparison of the depletion efficiency in random mode for HL-LHC V1.3 and HL-LHC V1.4.

Pulsed mode The HEL operation in pulsed mode is simulated over a grid of 20×20 , probing all possible combinations of the number of turns on and off between 1 and 20. The total number of turns simulated corresponds to 10 s in HL-LHC. The result is illustrated in Fig. 4. The most remarkable feature in both figures is the clear and distinct periodicity $T = i$ (turns ON) + j (turns OFF) for which the depletion efficiency is maximized. For HL-LHC V1.3, this

periodicity is $T = 23$ turns, for HL-LHC V1.4 it is $T = 24$ turns. Furthermore, in both cases additional lines at higher harmonics are visible. For example, for HL-LHC V1.4, clear areas of increased depletion efficiency can be identified at $T = 12$, half of the most efficient periodicity, and also at $T = 20$, at 5/6 of the most efficient periodicity. For the periodicity of 23, the second harmonic cannot be simulated because it does not correspond to an integer. However, we see clear and distinct lines in the proximity at $T = 13$ and $T = 11$. Another difference is the depletion fraction achieved over 10 s. For HL-LHC V1.3, the highest depletion fraction achieved is 20% with $T = 23$. For HL-LHC V1.4, the highest depletion fraction is 34% with $T = 24$.

These findings altogether indicate that the peaks of depletion in the pulsed operation are caused by a resonant effect from the interaction of particles with the HEL. With the update of the optics, the resonant periodicity has moved from $T = 23$ to $T = 24$. Further studies, outside of the scope of this contribution, showed a large variation of the peak depletion rate in pulsed operation with octupole current. This is in line with the hypothesis that the difference in the peak depletion rate and the resonance periodicity between the two optics can potentially be drawn back to a change of the shape of the phase space area taking into account the non-linearities. Current studies attempting to further explain this resonant behavior are ongoing.

Assessment of Effects on the Core

Emittance growth is studied for the random mode, which was found to be the most critical operational mode in [13]. The results for both optics versions are shown in Fig. 5. The initial distribution as a single Gaussian with an initial emittance of $2.5 \mu\text{m rad}$. The number of tracked particles is set to 30000 and the RMS emittance is inferred from the observed distribution of particles every second. We also show the rolling mean over five data points, corresponding to 5 s, to average over the fluctuating data. To estimate the difference in emittance growth for the two scenarios, we perform a linear regression on the calculated emittances (not on the rolling mean) over time for both cases. In view of the induced emittance growth, it is envisaged to operate the HEL with this pulsing over only five minutes, corresponding to approximately 3.4 million turns. The simulated results of the emittance growth over five minutes, inferred from the linear regressions, are listed in Table 3.

The growth rate simulated for V1.4 is approximately 28% larger than for V1.3 (the change of vertical β -function is 33%). While the pulsing of the electron lens was random with a probability of being switched on/off of 50% in both cases, the precise sequence of turns at which the lens was switched on or off was different in the two simulation cases. This difference, however, should average out over time and should not be significant for a simulation over two million turns. If we take into account that the growth of the emittance can be attenuated by a factor of approximately 15 with the transverse damper system (ADT) [21, 22], the total emittance

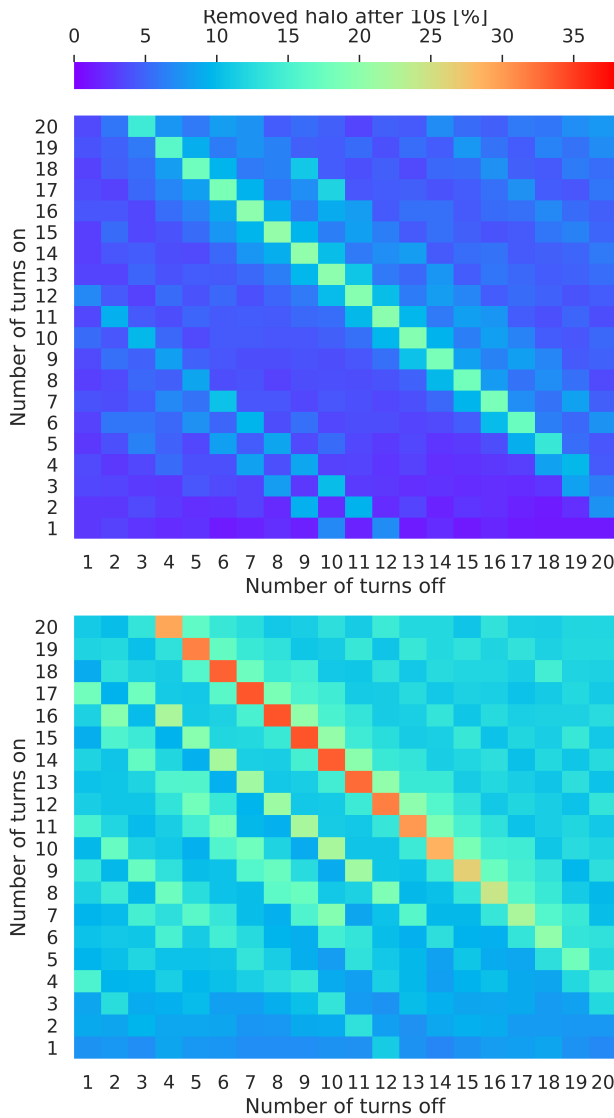


Figure 4: Depletion efficiency over 10 s of operation of the HEL in pulsed mode. The vertical axis corresponds to i , the horizontal axis to j . Top: HL-LHC V1.3, bottom: V1.4.

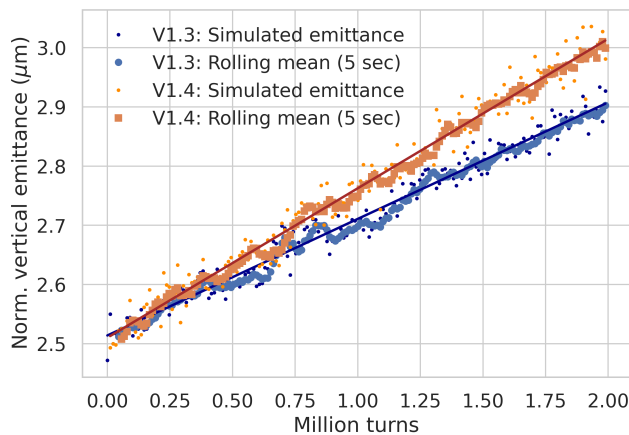


Figure 5: Simulated emittance evolution with a residual vertical dipole kick of 1 nrad for both optics versions, without considering the attenuating effect from the ADT.

growth after five minutes of operation is in the order of 0.04 to 0.06 $\mu\text{m rad}$ for the two optics studied, as listed in Table 3. We deem both as tolerable, considering that it is a onetime effect per fill. Note also, that the studied scenario assumes the HEL to be operated at the maximum current. With lower electron beam currents, the residual dipole kick and the emittance growth will be lower than presented above.

Table 3: Simulated vertical emittance growth for HL-LHC optics V1.3 and V1.4 assuming a residual kick of 1 nrad, operating the HEL with random pulsing over 5 minutes, with and without effect from the ADT. It is assumed that the ADT attenuates the emittance growth by a factor of 15.

Optics	$\Delta\epsilon_y$ ($\mu\text{m rad}$) in 5 minutes	
	Without ADT	With ADT
V1.3	0.65	0.04
V1.4	0.85	0.06

CONCLUSIONS

Hollow electron lenses are crucial building blocks for the safe and successful operation of the HL-LHC. The key performance indicator for the beam dynamics with HELs is the depletion efficiency. At the same time, the beam-core emittance growth due to residual dipole fields must be minimized. The studies presented in this paper have illustrated that the efficiency of depletion in the relevant modes, without beam-beam interaction, is similar for the two optics considered: the previous HL-LHC baseline and a new version optimized for the HEL. While the efficiency in constant current mode is insufficient to meet the requirements with separated beams with both optics versions, operation in the random mode delivers a promising depletion fraction. Depletion patterns observed in pulsed operation for both optics versions show the same qualitative key features, but at different pulsing periodicity. This behaviour may be caused by a change in the shape of the phase space and is currently under investigation. Further studies are ongoing to assess the impact of beam-beam interactions on the halo depletion efficiency of HELs. The emittance growth induced by the random mode is slightly larger in V1.4 than in V1.3, which can be qualitatively explained by the larger local β -functions. It can be reduced with the ADT to a sufficiently low level in both cases. Overall, the results let us conclude that the update of optics, motivated by better electron beam stability, symmetry between the two transverse planes and relaxed requirements for tolerances on electron and hadron beams, allows us to maintain similar depletion efficiencies for the relevant operational modes without inducing a strong deterioration in terms of emittance growth.

ACKNOWLEDGMENTS

The authors would like to express their gratitude for the support from the HL-LHC project. We thank G. Iadarola for his support in setting up the XSuite environment.

REFERENCES

- [1] G. Apollinari *et al.*, “High-Luminosity Large Hadron Collider (HL-LHC): Technical Design Report V. 0.1,” 2017, doi:10.23731/CYRM-2017-004
- [2] O. S. Brüning *et al.*, “LHC design report v.1 : The LHC main ring,” *CERN-2004-003-V1*, 2004.
- [3] R. W. Assmann *et al.*, “The Final Collimation System for the LHC,” in *Proc. 10th European Particle Accelerator Conf. (EPAC’06)*, Edinburgh, UK, 2006, pp. 986–988, <https://jacow.org/e06/papers/tuodfi01.pdf>
- [4] R.W. Assmann, “Collimators and Beam Absorbers for Cleaning and Machine Protection,” in *Proceedings of the LHC Project Workshop - Chamonix XIV*, Chamonix, France, 2005, pp. 261–267, <https://cds.cern.ch/record/987838>
- [5] R. Bruce *et al.*, “Simulations and measurements of beam loss patterns at the CERN Large Hadron Collider,” *Phys. Rev. ST Accel. Beams*, vol. 17, p. 081004, 8 2014, doi:10.1103/PhysRevSTAB.17.081004
- [6] S. Redaelli *et al.*, “High-Luminosity Large Hadron Collider (HL-LHC): Technical design report, Chapter 5: Collimation System,” 2020, doi:10.23731/CYRM-2020-0010.87
- [7] G. Valentino *et al.*, “Beam diffusion measurements using collimator scans in the LHC,” *Phys. Rev. ST Accel. Beams*, vol. 16, p. 021003, 2 2013, doi:10.1103/PhysRevSTAB.16.021003
- [8] A. Gorzawski *et al.*, “Probing LHC halo dynamics using collimator loss rates at 6.5 TeV,” *Phys. Rev. Accel. Beams*, vol. 23, p. 044802, 2020, doi:10.1103/PhysRevAccelBeams.23.044802
- [9] R. Appleby *et al.*, “Report from the review panel,” *Review of the needs for a hollow electron lens for the HL-LHC*, CERN, Geneva, Switzerland, 2016, <https://indico.cern.ch/event/567839/overview>
- [10] B. Lindstrom *et al.*, “Fast failures in the LHC and the future high luminosity LHC,” *Phys. Rev. Accel. Beams*, vol. 23, p. 081001, 8 2020, doi:10.1103/PhysRevAccelBeams.23.081001
- [11] S. Redaelli *et al.*, “Hollow electron lenses for beam collimation at the High-Luminosity Large Hadron Collider (HL-LHC),” *J. Instrum.*, vol. 16, no. 03, P03042, 2021, doi:10.1088/1748-0221/16/03/p03042
- [12] R. Bruce *et al.*, “Functional and operational conditions of the Hollow Electron Lenses (HEL) at HL-LHC,” *CERN EDMS 2514085*, 2021.
- [13] D. Mirarchi *et al.*, “Nonlinear dynamics of proton beams with hollow electron lens in the CERN High-Luminosity LHC,” *Submitted to European Physical Journal Plus*, 2021.
- [14] A. Mereghetti, “Status of Simulations and Required Inputs,” 2019, Presentation at the 122nd Collimation Upgrade Specification Meeting, ColUSM, 22/11/2019, CERN, Switzerland.
- [15] *Sixtrack web site*, <https://sixtrack.web.cern.ch/SixTrack/>
- [16] R. De Maria *et al.*, “SixTrack Version 5: Status and New Developments,” in *Proc. IPAC’19*, Melbourne, Australia, 2019, pp. 3200–3203, doi:10.18429/JACoW-IPAC2019-WEPTS043
- [17] R. Bruce *et al.*, “Status of SixTrack with collimation,” in *Proceedings of the ICFA Mini-Workshop on Tracking for Collimation*, CERN, Geneva, Switzerland, 2018, p. 10, doi:10.23732/CYRCP-2018-002.1
- [18] G. Iadarola *et al.*, *Xsuite website*, <https://xsuite.readthedocs.io/en/latest/>
- [19] R. D. Maria *et al.*, “SixTrack Project: Status, Runtime Environment, and New Developments,” in *Proc. ICAP’18*, Key West, FL, USA, 2019, pp. 172–178, doi:10.18429/JACoW-ICAP2018-TUPAF02
- [20] P. Racano *et al.*, “Review of halo measurements at LHC with collimator scans,” Presentation at the HL-LHC Collaboration Meeting, 15-18 October 2018, Geneva, Switzerland.
- [21] W. Hofle *et al.*, “LHC Transverse Feedback System and its Hardware Commissioning,” in *Proc. EPAC’08*, Genoa, Italy, 2008, pp. 3266–3268, <https://jacow.org/e08/papers/thpc121.pdf>
- [22] X. Buffat *et al.*, “Modeling of the emittance growth due to decoherence in collision at the Large Hadron Collider,” *Phys. Rev. Accel. Beams*, vol. 23, p. 021002, 2020, doi:10.1103/PhysRevAccelBeams.23.021002